Comp. & Maths. with Appls. Vol. 6, pp. 235–245

0097–4943/80/0601–0235/$02.00/0

NUMERICAL SOLUTION OF A MICROPOLAR FLOW BETWEEN A ROTATING AND A STATIONARY DISC

M. ANWAR and G. S. GURAM

Department of Applied Mathematics, University of Western Ontario, London, Canada

Communicated by E. Y. Rodin

(*Received February* 1979)

Abstract—The steady flow of a micropolar fluid between two infinite discs, when one is held at rest and the other rotating with constant angular velocity, is considered. The equations of motion are reduced to a system of ordinary differential equations, which in turn are solved numerically using the Gauss–Seidel iterative procedure and Simpson's rule, for four different combinations of the seven parameters involved. Results are given both in tabular and graphical form, and compared with the known theoretical results.

1. INTRODUCTION

The theory of micropolar fluids[5] has received considerable attention in recent years, the extent of which can be judged from the comprehensive review by Smith[15]. Poiseuille flow has been considered by Eringen[5], Condiff and Dahler[6] and Aero, Bulygin and Kuvshinskii[4]; Couette flow by Condiff and Dahler[6]. The micropolar model has been used to describe the flow of liquid crystals[7].

Singh and Smith[8] investigated the steady porous plane Couette and Poiseuille flows of a micropolar fluid. They found, for certain ranges of the rate of suction and injection, that the velocity is composed of a linear combination of real exponential terms, whereas for other values products of exponentials and sinusoidal terms occur, provided the material constants satisfy certain inequalities.

Smith and Guram[10] considered the two-dimensional incompressible motions of a micropolar fluid, in which the vorticity and spin are constant along a streamline at any time, are shown to be one of two types, and particular solutions obtained in a number of cases.

Guram and Smith[11] investigated the flow of a micropolar fluid bounded by a rigid wall moving with speed proportional to t^n parallel to itself, with injection proportional to $t^{-1/2}$. The first two terms of a perturbation expansion for speed and spin in powers of t, with coefficients which are functions of $\eta \propto yt^{-1/2}$, were obtained, when the material constants satisfy the relation $(\mu + \kappa)j = \gamma$.

Guram and Smith[12] established the uniqueness and existence of rectilinear flow of a micropolar fluid, through a pipe of arbitrary cross-section, with no slip at the boundary, and a perturbation expansion obtained for flow through an elliptic pipe. They suggested a method of estimating the material constants, when the coupling constant is small.

Smith and Guram[13] considered the flow of a micropolar fluid, which is steady relative to a frame of reference rotating with small uniform angular velocity, when the velocity and spin are two-dimensional and depend only on the depth, and the pressure is independent of the horizontal co-ordinates. They obtained the orientation of the velocity, spin, stress and couple-stress vectors on the surface and the flow is determined when the surface is free from the couple stress.

The problem of rotating disc for Newtonian fluids has been considered by Kármán[1] and Cochran[2]. Datta and Sastry[14] considered the flow of a micropolar fluid between two infinite slowly rotating disks and obtained the series solutions in terms of the Reynolds number of the motion.

In this paper, the flow of a micropolar fluid contained between two infinite discs, when one is held at rest and the other is rotating with constant angular velocity about their common axis, is considered. The specific equations of motion are stated in Section 2. In Section 3, the equations of motion are reduced to seven ordinary differential equations, involving seven parameters. In Section 4, the finite-difference equations are given. The computational procedure is presented in Section 5. In Section 6, the numerical results are presented both in tabular and graphical form, and compared with the known theoretical results[14].

2. EQUATIONS OF MOTION

The equations of motion of a micropolar fluid are[5]

$$\frac{\partial \rho}{\partial t} + \nabla \cdot (\rho \mathbf{v}) = 0, \tag{2.1}$$

$$(\lambda + 2\mu + \kappa)\nabla(\nabla \cdot \mathbf{v}) - (\mu + \kappa)\nabla \times \nabla \times \mathbf{v} + \kappa \nabla \times \boldsymbol{\nu} - \nabla p + \rho \mathbf{f} = \rho \dot{\mathbf{v}}, \tag{2.2}$$

$$(\alpha + \beta + \gamma)\nabla(\nabla \cdot \boldsymbol{\nu}) - \gamma(\nabla \times \nabla \times \boldsymbol{\nu}) + \kappa \nabla \times \mathbf{v} - 2\kappa \boldsymbol{\nu} + \rho \mathbf{l} = \rho j \dot{\boldsymbol{\nu}}, \tag{2.3}$$

where ρ is the density, $\mathbf{v}$ the velocity, $\boldsymbol{\nu}$ the micro-rotation or spin, p the thermo-dynamic pressure, $\mathbf{f}$ and $\mathbf{l}$ the body force and couple per unit mass, and j the micro-inertia; α, β, γ, λ, μ, and κ are material constants (viscosity coefficients); and the dot signifies material differentiation.

The constitutive equations, giving the stress tensor t_{kl} and the couple stress tensor m_{kl}, are (in curvilinear co-ordinates)

$$t_{kl} = (-p + \lambda v_{r;r})g_{kl} + \mu(v_{k;l} + v_{l;k}) + \kappa(v_{l;k} - \epsilon_{klr}\nu_r), \tag{2.4}$$

$$m_{kl} = \alpha \nu_{r;r} g_{kl} + \beta \nu_{k;l} + \gamma \nu_{l;k}, \tag{2.5}$$

where g_{kl} and ϵ_{klr} are the metric tensor and the covariant ϵ-symbol, respectively. The semi-colon denotes the covariant partial differentiation with respect to a space co-ordinate and repeated indices are summed. The stress vector $\mathbf{t}$ and couple stress vector $\mathbf{m}$ at a point on a surface with normal $\mathbf{n}$ are given by $t_{\alpha k} n_\alpha = t_k$ and $m_{\alpha k} n_\alpha = m_k$. The material constants must satisfy the following inequalities, derived from the Clausius–Duhem inequality:

$$3\lambda + 2\mu + \kappa \geq 0, 2\mu + \kappa \geq 0, \kappa \geq 0, 3\alpha + \beta + \gamma \geq 0, \gamma \geq |\beta|. \tag{2.6}$$

The boundary conditions assumed are $\mathbf{v}(x_B, t) = \mathbf{v}_B$, $\boldsymbol{\nu}(x_B, t) = \boldsymbol{\nu}_B$ where x_B is a point on a rigid boundary with prescribed velocity $\mathbf{v}_B$ and spin $\boldsymbol{\nu}_B$. That is, we assume neither slip nor spin at a fixed boundary. Other possible boundary conditions are discussed in [4] and [6].

3. FLOW BETWEEN A STATIONARY AND A ROTATING DISC

We consider the flow of a micropolar fluid between two infinite co-axial discs, at a finite distance h_1 apart from each other. The fluid motion is induced due to the motion of the lower disc which is rotating with constant angular velocity Ω. We use the cylindrical polar co-ordinate r, θ, z system, where $r = 0$ is the axis of the rotation of the plane of the lower disc. We assume that the material constants of the micropolar fluid are independent of position and neglect body forces and body couples. We, also, assume that the flow is steady, incompressible and axially-symmetric, and so we look for a solution for which

$$\begin{aligned} \mathbf{v} &= (u(r, z), v(r, z), w(r, z)), \\ \boldsymbol{\nu} &= (\nu_1(r, z), \nu_2(r, z), \nu_3(r, z)). \end{aligned} \tag{3.1}$$

Substituting (3.1) in (2.1), (2.2) and (2.3), we obtain

$$\frac{1}{r}\frac{\partial}{\partial r}(ru) + \frac{\partial w}{\partial z} = 0, \tag{3.2}$$

$$(\mu + \kappa)\left(\frac{\partial^2 u}{\partial r^2} + \frac{1}{r}\frac{\partial u}{\partial r} + \frac{\partial^2 u}{\partial z^2} - \frac{u}{r^2}\right) - \kappa \frac{\partial \nu_2}{\partial z} - \frac{\partial p}{\partial r} = \rho\left(\frac{w \partial u}{\partial z} - \frac{v^2}{r} + \frac{u \partial u}{\partial r}\right), \tag{3.3}$$

$$(\mu + \kappa)\left(\frac{\partial^2 v}{\partial r^2} + \frac{1}{r}\frac{\partial v}{\partial r} + \frac{\partial^2 v}{\partial z^2} - \frac{v}{r^2}\right) + \kappa\left(\frac{\partial \nu_1}{\partial z} - \frac{\partial \nu_3}{\partial r}\right) = \rho\left(\frac{w \partial v}{\partial z} + \frac{uv}{r} + \frac{u \partial v}{\partial r}\right), \tag{3.4}$$

$$(\mu+\kappa)\left(\frac{\partial^2 w}{\partial r^2}+\frac{1}{r}\frac{\partial w}{\partial r}+\frac{\partial^2 w}{\partial z^2}\right)+\frac{\kappa}{r}\frac{\partial}{\partial r}(r\nu_2)-\frac{\partial p}{\partial z}=\rho\left(\frac{u\partial w}{\partial r}+\frac{w\partial w}{\partial z}\right), \tag{3.5}$$

$$\begin{aligned}(\alpha+\beta+\gamma)\frac{\partial}{\partial r}\left(\frac{\partial \nu_1}{\partial r}+\frac{\nu_1}{r}+\frac{\partial \nu_3}{\partial z}\right)-\gamma\frac{\partial}{\partial z}\left(\frac{\partial \nu_3}{\partial r}-\frac{\partial \nu_1}{\partial z}\right)-\kappa\frac{\partial v}{\partial z}-2k\nu_1\\ =\rho j\left(u\frac{\partial \nu_1}{\partial r}-\frac{1}{r}v\nu_2+w\frac{\partial \nu_1}{\partial z}\right),\end{aligned} \tag{3.6}$$

$$\gamma\left[\frac{\partial}{\partial r}\left(\frac{\partial \nu_2}{\partial r}+\frac{\nu_2}{r}\right)+\frac{\partial^2 \nu_2}{\partial z^2}\right]+\kappa\left(\frac{\partial u}{\partial z}-\frac{\partial w}{\partial r}\right)-2\kappa\nu_2=\rho j\left(\frac{u\partial \nu_2}{\partial r}+\frac{1}{r}v\nu_1+\frac{w\partial \nu_2}{\partial z}\right), \tag{3.7}$$

and

$$\begin{aligned}(\alpha+\beta+\gamma)\frac{\partial}{\partial z}\left(\frac{\partial \nu_1}{\partial r}+\frac{\nu_1}{r}+\frac{\partial \nu_3}{\partial z}\right)-\gamma\frac{1}{r}\frac{\partial}{\partial r}\left[r\left(\frac{\partial \nu_1}{\partial z}-\frac{\partial \nu_3}{\partial r}\right)\right]+\frac{\kappa}{r}\frac{\partial}{\partial r}(rv)-2\kappa\nu_3\\ =\rho j\left(\frac{u\partial \nu_3}{\partial r}+\frac{w\partial \nu_3}{\partial z}\right).\end{aligned} \tag{3.8}$$

The boundary conditions are

$$\begin{aligned}\text{when } z=0; \quad & u=0,\ v=r\Omega,\ w=0,\\ & \nu_1=0,\ \nu_2=0,\ \nu_3=0,\ p=0,\end{aligned} \tag{3.9}$$

$$\text{and when } z=h_1; \quad u=0,\ v=0,\ \nu_1=\nu_2=\nu_3=0. \tag{3.10}$$

Using the dimensional analysis, the velocity, the micro-rotation and the pressure are assumed to be of the form:

$$\begin{aligned}&u=r\Omega F_1(\eta),\ v=r\Omega F_2(\eta),\ w=h_1\Omega F_3(\eta),\\ &\nu_1=\frac{r\Omega}{h_1}G_1(\eta),\ \nu_2=\frac{r\Omega}{h_1}G_2(\eta),\ \nu_3=\Omega G_3(\eta),\\ &p=p(z)=-(\mu+\kappa)\Omega P(\eta),\end{aligned} \tag{3.11}$$

where

$$\eta=\frac{z}{h_1}. \tag{3.12}$$

If we substitute (3.11) into the eqns (3.2)–(3.8), then after some calculations we obtain the following seven ordinary differential equations:

$$2F_1+F_3'=0, \tag{3.13}$$

$$F_1''-\eta_1 G_2'=\eta_2(F_3F_1'-F_2^2+F_1^2), \tag{3.14}$$

$$F_2''+\eta_1 G_1'=\eta_2(F_3F_2'+2F_1F_2), \tag{3.15}$$

$$F_3''+2\eta_1 G_2+P'=\eta_2 F_3F_3', \tag{3.16}$$

$$G_1''-\eta_3 F_2'-2\eta_3 G_1=\eta_4(F_1G_1-F_2G_2+F_3G_1'), \tag{3.17}$$

$$G_2''+\eta_3 F_1'-2\eta_3 G_2=\eta_4(F_1G_2+F_2G_1+F_3G_2'), \tag{3.18}$$

$$G_3'' + 2\eta_5 G_1' + 2\eta_6(F_2 - G_3) = \eta_7 F_3 G_3', \tag{3.19}$$

where the prime denotes differentiation with respect to η, and

$$\eta_1 = \frac{\kappa}{\mu + \kappa}, \eta_2 = \frac{\rho\Omega h_1^2}{\mu + \kappa}, \eta_3 = \frac{\kappa h_1^2}{\gamma},$$

$$\eta_4 = \frac{\rho j\Omega h_1^2}{\gamma}, \eta_5 = \frac{\alpha + \beta}{\alpha + \beta + \gamma}, \eta_6 = \frac{\kappa h_1^2}{\alpha + \beta + \gamma}, \tag{3.20}$$

$$\eta_7 = \frac{\rho j\Omega h_1^2}{\alpha + \beta + \gamma},$$

and we note that all of these are dimensionless. The dimensions of the above parameters are as follows:

$$[\mu, \kappa] = ML^{-1}T^{-1}, [\alpha, \beta, \gamma] = MLT^{-1},$$

$$[j] = L^2, [\Omega] = T^{-1}, [h_1] = L, \tag{3.21}$$

$$[\rho] = ML^{-3}.$$

The boundary conditions (3.9) and (3.10), in the new independent variable become

$$\begin{aligned} &\eta = 0: \ F_1 = 0, F_2 = 1, F_3 = 0, G_1 = G_2 = G_3 = 0, P = 0, \\ &\eta = 1: \ F_1 = F_2 = 0, G_1 = G_2 = G_3 = 0. \end{aligned} \tag{3.22}$$

4. FINITE-DIFFERENCE EQUATIONS

The interval $[0, 1]$ considered is divided into grid points with uniform spacing h. A typical grid point is denoted by η_i. The eqns (3.14), (3.15), (3.17)–(3.19) are approximated by replacing all derivatives by central-difference approximations. The resulting finite-difference equations are the following:

$$F_{i-1}^{(1)} - 2F_i^{(1)} + F_{i+1}^{(1)} = \frac{\eta_1 h}{2}(G_{i+1}^{(2)} - G_{i-1}^{(2)}) + \eta_2\left[\frac{1}{2}F_i^{(3)}h(F_{i+1}^{(1)} - F_{i-1}^{(1)}) - h^2F_i^{(2)}F_i^{(2)} + h^2F_i^{(1)}F_i^{(1)}\right], \tag{4.1}$$

$$F_{i-1}^{(2)} - 2F_i^{(2)} + F_{i+1}^{(2)} = -\frac{1}{2}\eta_1 h(G_{i+1}^{(1)} - G_{i-1}^{(1)}) + \eta_2\left[\frac{1}{2}F_i^{(3)}h(F_{i+1}^{(2)} - F_{i-1}^{(2)}) + 2h^2F_i^{(1)}F_i^{(2)}\right], \tag{4.2}$$

$$G_{i-1}^{(1)} - 2(1 + h^2\eta_3)G_i^{(1)} + G_{i+1}^{(1)} = \eta_3\frac{h}{2}(F_{i+1}^{(2)} - F_{i-1}^{(2)}) + \eta_4[h^2F_i^{(1)}G_i^{(1)} - h^2F_i^{(2)}G_i^{(2)} + \frac{h}{2}F_i^{(3)}(G_{i+1}^{(1)} - G_{i-1}^{(1)})\Big], \tag{4.3}$$

$$G_{i-1}^{(2)} - 2(1 + \eta_3h^2)G_i^{(2)} + G_{i+1}^{(2)} = -\frac{\eta_3 h}{2}(F_{i+1}^{(1)} - F_{i-1}^{(1)}) + \eta_4[h^2F_i^{(1)}G_i^{(2)} + h^2F_i^{(2)}G_i^{(1)} + \frac{h}{2}F_i^{(3)}(G_{i+1}^{(2)} - G_{i-1}^{(2)})\Big], \tag{4.4}$$

and

$$G_{i-1}^{(3)} - 2(1+\eta_6 h^2)G_i^{(3)} + G_{i+1}^{(3)} = -\eta_5 h(G_{i+1}^{(1)} - G_{i-1}^{(1)}) - 2h^2\eta_6 F_i^{(2)} + \frac{1}{2}h\eta_7 F_i^{(3)}(G_{i+1}^{(3)} - G_{i-1}^{(3)}), \tag{4.5}$$

which are solved for all grid points interior to the interval [0, 1] with conditions (3.22) on F_1, F_2, G_1, G_2 and G_3 at the end points. The first-order eqns (3.13) and (3.16) are integrated using the prescribed conditions (3.22) on F_3 and P.

5. COMPUTATIONAL PROCEDURE

Now, we need to solve the above system of finite-difference equations at each required grid point. Each set of equations is solved in turn, subject to the appropriate boundary conditions, using the Gauss-Seidel iterative procedure [9, pp. 154–156], whereas the equations (3.13) and (3.16) are integrated using the Simpson's rule [9, pp. 67–69] with the formula given in [3, pp. 48] and the conditions on F_3 and P.

The iterative sequence is as follows:

(1) The equations (4.1) are solved subject to $F_1 = 0$ when $\eta = 0$ and $\eta = 1$, using the most recently available values for F_1, F_2, F_3, and G_2 to calculate the elements of the matrix associated with F_1. Then the eqn (3.13) is solved by the Simpson's rule with $F_3 = 0$ when $\eta = 0$;

(ii) the computed solution for F_1 and F_3 is introduced into (4.2) and these equations are solved subject to $F_2 = 1$ at $\eta = 0$ and $F_2 = 0$ at $\eta = 1$. The most recently available information for F_1, F_2, F_3 and G_1 is again used for calculating the values of F_2;

(iii) the solutions for F_1, F_2 and F_3 are introduced into (4.3)–(4.5), and these sets of equations are solved for G_1, G_2 and G_3 respectively, subject to $G_1 = G_2 = G_3 = 0$ when $\eta = 0$, and $\eta = 1$, using the recent values for F_1, F_2, F_3, G_1, G_2 and G_3. The solutions for these equations provide updated information for the subsequent application of (i) and (ii).

The above procedure is repeated until all the solutions have approached to some required criterion of accuracy. The criterion

$$|F_i^{(n+1)} - F_i^{(n)}| < 10^{-6}, |G_i^{(n+1)} - G_i^{(n)}| < 10^{-6},$$

where $i = 1, 2, 3$, was adopted as a terminating condition, where here the subscript denotes the number of a function and the superscript the iteration.

The computed solutions of F_1, F_3 and G_2 were introduced to solve (3.16) to calculate the pressure with $P = 0$ when $\eta = 0$.

6. RESULTS AND DISCUSSION

The results have been obtained for the following four cases:

	η_1	η_2	η_3	η_4	η_5	η_6	η_7
Case 1	0.3	0.8	0.2	0.02	0.5	0.08	0.01
Case 2	0.45	1.4	0.3	0.03	0.85	0.12	0.015
Case 3	0.6	1.6	0.4	0.04	1.0	0.16	0.02
Case 4	0.75	2.333	0.5	0.05	1.417	2.4	0.25

The calculations were carried out for two different grid sizes, namely (a) $h = 0.025$; (b) $h = 0.0125$. The accuracy of the results may be checked by comparing the results on the different grid sizes. For this comparison, in Tables 1–4, the values of F_1, F_2, F_3, G_1, G_2, G_3 and P are given for the cases considered. The general trend of these results as the grid size is decreased tends to indicate that the solutions for $h = 0.0125$ are accurate to within a 0.03% tolerance for F_1, F_2, F_3, G_1, G_2, G_3 and 0.33% for P.

Typical sets of solutions, showing the effects of the parameters η_1, η_2, η_3, η_4, η_5, η_6 and η_7 are given in graphical form in Figs. 1–7. For all the four cases considered, it was found that as

Table 1.

Grid Size	η	F_1	F_2	F_3	G_1	G_2	G_3	P
$\frac{1}{40}$	0.0	0.0	1.0	0.0	0.0	0.0	0.0	0.0
	0.1	0.0160952	0.8987063	-0.0017296	0.0087350	0.0002138	0.0056283	0.0320491
	0.2	0.0257190	0.7974170	-0.0060070	0.0154781	0.0001750	0.0090536	0.0513258
	0.3	0.0302414	0.6963258	-0.0116775	0.0202584	-0.0000002	0.0106414	0.0604302
	0.4	0.0308708	0.5955478	-0.0178444	0.0231003	-0.0002223	0.0107509	0.0617903
	0.5	0.0286524	0.4951491	-0.0238363	0.0240224	-0.0004252	0.0097365	0.0574913
	0.6	0.0244675	0.3951687	-0.0291746	0.0230362	-0.0005621	0.0079485	0.0492796
	0.7	0.0190340	0.2956339	-0.0335405	0.0201467	-0.0006023	0.0057348	0.0385694
	0.8	0.0129079	0.1965713	-0.0367424	0.0153515	-0.0005273	0.0034414	0.0264499
	0.9	0.0064843	0.0980130	-0.0386841	0.0084414	-0.0003278	0.0014142	0.0136925
	1.0	0.0000000	0.0000000	-0.0393324	0.0000000	-0.0000000	0.0000000	0.0007556
$\frac{1}{80}$	0.0	0.0	1.0	0.0	0.0	0.0	0.0	0.0
	0.1	0.0160981	0.8987067	-0.0017299	0.0087352	0.0002136	0.0056283	0.0321558
	0.2	0.0257241	0.7974176	-0.0060081	0.0154784	0.0001747	0.0090537	0.0514155
	0.3	0.0302481	0.6963262	-0.0116798	0.0202588	-0.0000006	0.0106415	0.0605043
	0.4	0.0308784	0.5955479	-0.0178481	0.0231008	-0.0002228	0.0107510	0.0618499
	0.5	0.0286603	0.4951490	-0.0238416	0.0240228	-0.0004258	0.0097365	0.0575378
	0.6	0.0244750	0.3951683	-0.0291815	0.0230366	-0.0005627	0.0079486	0.0493143
	0.7	0.0190406	0.2956334	-0.0335487	0.0201470	-0.0006028	0.0057348	0.0385934
	0.8	0.0129129	0.1965708	-0.0367518	0.0153518	-0.0005277	0.0034414	0.0264647
	0.9	0.0064871	0.0980127	-0.0386943	0.0086415	-0.0003280	0.0014142	0.0136993
	1.0	0.0000000	0.0000000	-0.0393429	0.0000000	-0.0000000	0.0000000	0.0007561

Table 2.

Grid Size	η	F_1	F_2	F_3	G_1	G_2	G_3	P
$\frac{1}{40}$	0.0	0.0	1.0	0.0	0.0	0.0	0.0	0.0
	0.1	0.0275956	0.8959168	-0.0029689	0.0130191	0.0005429	0.0094652	0.0549328
	0.2	0.0439407	0.7920250	-0.0102888	0.0229936	0.0004391	0.0148487	0.0876940
	0.3	0.0514764	0.6888571	-0.0199586	0.0299977	-0.0000096	0.0169239	0.1029939
	0.4	0.0523472	0.5867083	-0.0304357	0.0341004	-0.0005737	0.0164426	0.1051695
	0.5	0.0483961	0.4857258	-0.0405767	0.0353595	-0.0010851	0.0141370	0.0978791
	0.6	0.0411646	0.3859758	-0.0495761	0.0338191	-0.0014268	0.0107238	0.0841246
	0.7	0.0318966	0.2874903	-0.0569074	0.0295078	-0.0015229	0.0069076	0.0662897
	0.8	0.0215448	0.1902986	-0.0622631	0.0224383	-0.0013293	0.0033856	0.0461774
	0.9	0.0107796	0.0944453	-0.0654983	0.0126082	-0.0008243	0.0008515	0.0250440
	1.0	0.0000000	0.0000000	-0.0665746	0.0000000	-0.0000000	0.0000000	0.0036236
$\frac{1}{80}$	0.0	0.0	1.0	0.0	0.0	0.0	0.0	0.0
	0.1	0.0276008	0.8959180	-0.0029695	0.0130198	0.0005422	0.0094654	0.0551186
	0.2	0.0439498	0.7920261	-0.0102908	0.0229947	0.0004379	0.0148489	0.0878496
	0.3	0.0514881	0.6888575	-0.0199627	0.0299992	-0.0000113	0.0169241	0.1031214
	0.4	0.0523603	0.5867078	-0.0304423	0.0341021	-0.0005757	0.0164427	0.1052715
	0.5	0.0484095	0.4857245	-0.0405859	0.0353612	-0.0010871	0.0141370	0.0979580
	0.6	0.0411773	0.3859739	-0.0495880	0.0338207	-0.0014287	0.0107237	0.0841831
	0.7	0.0319075	0.2874883	-0.0569216	0.0295091	-0.0015246	0.0069074	0.0663302
	0.8	0.0215530	0.1902968	-0.0622793	0.0224393	-0.0013306	0.0033854	0.0462024
	0.9	0.0107842	0.0944442	-0.0655158	0.0126087	-0.0008250	0.0008514	0.0250558
	1.0	0.0000000	0.0000000	-0.0665926	0.0000000	-0.0000000	0.0000000	0.0036265

Table 3.

Grid Size	η	F_1	F_2	F_3	G_1	G_2	G_3	P
$\frac{1}{40}$	0.0	0.0	1.0	0.0	0.0	0.0	0.0	0.0
	0.1	0.0313062	0.8950813	-0.0033694	0.0171590	0.0008123	0.0131074	0.0622936
	0.2	0.0497864	0.7901738	-0.0116681	0.0302531	0.0006500	0.0203675	0.0993172
	0.3	0.0582368	0.6860302	-0.0226160	0.0394037	-0.0000284	0.0229402	0.1165291
	0.4	0.0591201	0.5830919	-0.0344591	0.0447248	-0.0008759	0.0219443	0.1189345
	0.5	0.0545536	0.4816058	-0.0459015	0.0463132	-0.0016401	0.0184623	0.1107266
	0.6	0.0463059	0.3817118	-0.0560359	0.0442432	-0.0021471	0.0135470	0.0953179
	0.7	0.0358007	0.2835042	-0.0642741	0.0385646	-0.0022853	0.0082291	0.0753929
	0.8	0.0241243	0.1870723	-0.0702788	0.0293019	-0.0019907	0.0035250	0.0529636
	0.9	0.0120394	0.0925244	-0.0738973	0.0164550	-0.0012325	0.0004448	0.0294186
	1.0	0.0000000	0.0000000	-0.0750983	0.0000000	-0.0000000	0.0000000	0.0055603
$\frac{1}{80}$	0.0	0.0	1.0	0.0	0.0	0.0	0.0	0.0
	0.1	0.0313129	0.8950837	-0.0033701	0.0171595	0.0008114	0.0131076	0.0625072
	0.2	0.0497983	0.7901768	-0.0116707	0.0302537	0.0006482	0.0203678	0.0994976
	0.3	0.0582522	0.6860330	-0.0226214	0.0394045	-0.0000308	0.0229406	0.1166783
	0.4	0.0591373	0.5830939	-0.0344678	0.0447257	-0.0008786	0.0219447	0.1190549
	0.5	0.0545711	0.4816070	-0.0459137	0.0463141	-0.0016430	0.0184628	0.1108208
	0.6	0.0463224	0.3817121	-0.0560515	0.0442440	-0.0021500	0.0135474	0.0953885
	0.7	0.0358147	0.2835039	-0.0642927	0.0385653	-0.0022878	0.0082295	0.0754426
	0.8	0.0241347	0.1870717	-0.0702999	0.0293025	-0.0019926	0.0035252	0.0529949
	0.9	0.0120450	0.0925239	-0.0739200	0.0164553	-0.0012336	0.0004449	0.0294338
	1.0	0.0000000	0.0000000	-0.0751215	0.0000000	-0.0000000	0.0000000	0.0055654

Table 4.

Grid Size	η	F_1	F_2	F_3	G_1	G_2	G_3	P
$\frac{1}{40}$	0.0	0.0	1.0	0.0	0.0	0.0	0.0	0.0
	0.1	0.0438845	0.8896312	-0.0047341	0.0215322	0.0013732	0.1056531	0.0872809
	0.2	0.0692998	0.7797176	-0.0163236	0.0377609	0.0010531	0.1681577	0.1382868
	0.3	0.0804668	0.6716677	-0.0315053	0.0489099	-0.0001416	0.1972851	0.1614697
	0.4	0.0810695	0.5662433	-0.0478073	0.0552059	-0.0016025	0.2010599	0.1643792
	0.5	0.0742326	0.4638088	-0.0634384	0.0568548	-0.0028966	0.1861118	0.1531291
	0.6	0.0625224	0.3645137	-0.0771766	0.0540282	-0.0037332	0.1579788	0.1325090
	0.7	0.0479641	0.2684174	-0.0882586	0.0468578	-0.0039332	0.1213706	0.1061464
	0.8	0.0320706	0.1755685	-0.0962743	0.0354346	-0.0033996	0.0803975	0.0766661
	0.9	0.0158801	0.0860502	-0.1010680	0.0198102	-0.0020914	0.0387736	0.0458231
	1.0	0.0000000	0.0000000	-0.1026479	0.0000000	-0.0000000	0.0000000	0.0145978
$\frac{1}{80}$	0.0	0.0	1.0	0.0	0.0	0.0	0.0	0.0
	0.1	0.0438946	0.8896343	-0.0047352	0.0215336	0.0013714	0.1056695	0.0875893
	0.2	0.0693174	0.7797206	-0.0163275	0.0377631	0.0010498	0.1681829	0.1385446
	0.3	0.0804891	0.6716689	-0.0315132	0.0489126	-0.0001462	0.1973136	0.1616804
	0.4	0.0810940	0.5662421	-0.0478199	0.0552088	-0.0016078	0.2010880	0.1645470
	0.5	0.0742571	0.4638056	-0.0634559	0.0568576	-0.0029021	0.1861369	0.1532588
	0.6	0.0625449	0.3645092	-0.0771989	0.0540307	-0.0037385	0.1579996	0.1326053
	0.7	0.0479829	0.2684124	-0.0882851	0.0468598	-0.0039379	0.1213861	0.1062141
	0.8	0.0320843	0.1755642	-0.0963040	0.0354360	-0.0034031	0.0804076	0.0767092
	0.9	0.0158875	0.0860476	-0.1010999	0.0198109	-0.0020934	0.0387784	0.0458453
	1.0	0.0000000	0.0000000	-0.1026805	0.0000000	-0.0000000	0.0000000	0.0146111

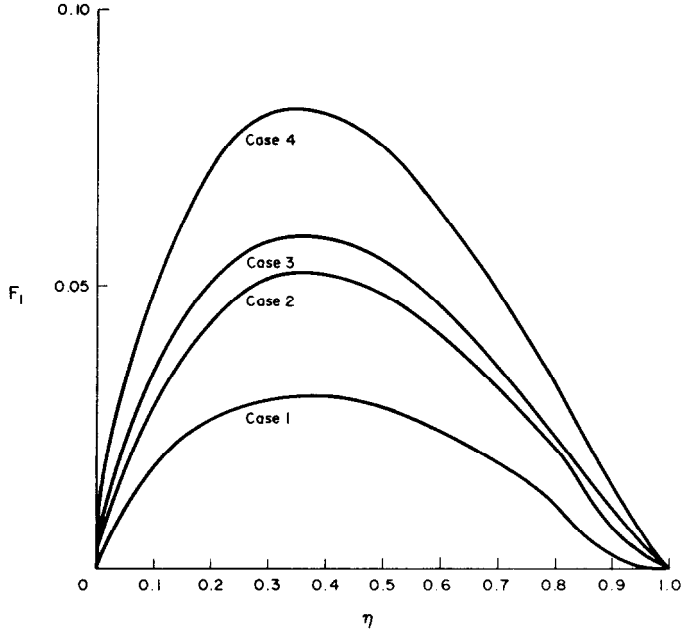
0.10
0.05
F_1
Case 4
Case 3
Case 2
Case 1
0
0.1
0.2
0.3
0.4
0.5
0.6
0.7
0.8
0.9
1.0
η

Fig. 1.

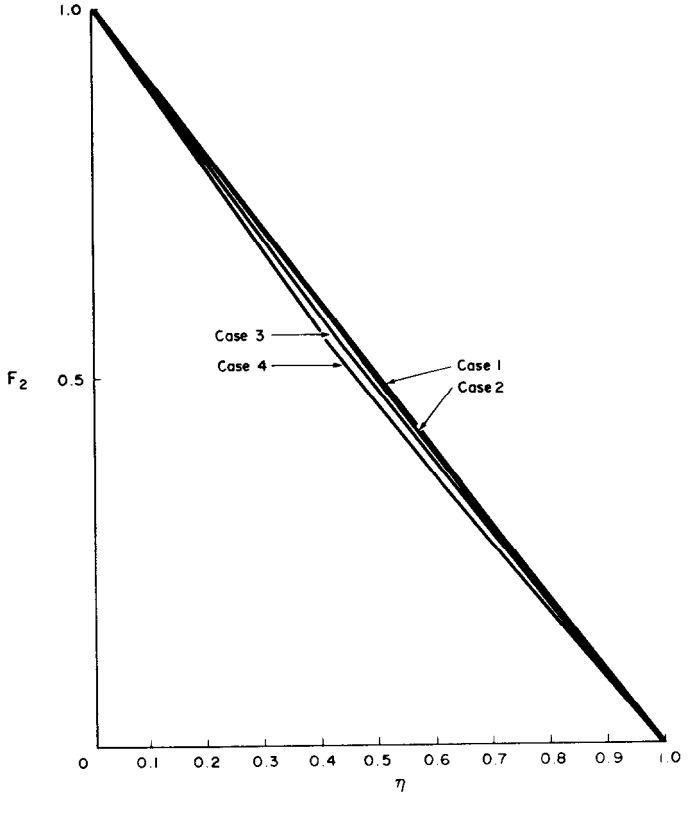
1.0
0.5
F_2
Case 3
Case 4
Case 1
Case 2
0
0.1
0.2
0.3
0.4
0.5
0.6
0.7
0.8
0.9
1.0
η

Fig. 2.

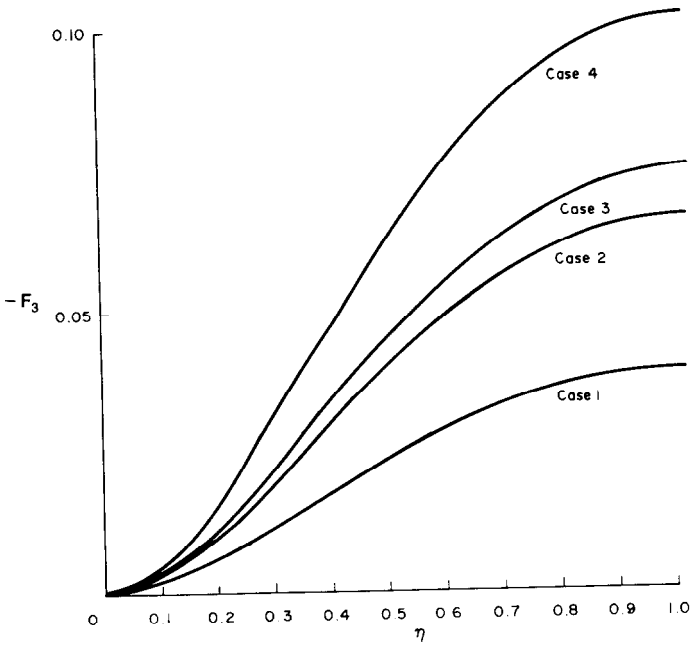

Fig. 3.

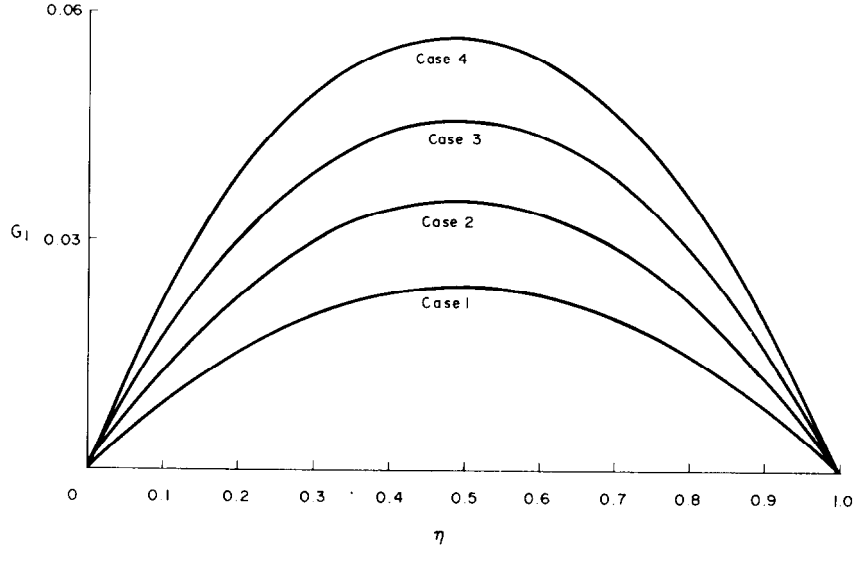

Fig. 4.

the parameters increase

(1) the profiles of F_1, G_1, G_3 and P were raised,

(2) the profiles of F_2 and F_3 were lowered,

(3) the profile of G_2 was raised between $\eta = 0$ and $\eta = 0.3$, and lowered between $\eta = 0.3$ and $\eta = 1.0$.

Figure 1 shows that F_1 is positive throughout between the two discs, showing thereby there is a radial outwards flow from the lower disc which is maximum at the plane $\eta = 0.4$ and starts approaching to zero towards the upper plate.

It is worthwhile to note here that in [14], F_1 is positive near the lower disc and negative near the upper disc because of the fact that in [14] the form of the pressure was taken to be dependent on two independent variables r and z, whereas in the present paper we followed the form as in [2]. Also in the present investigation, the terms involving micro-inertia are not neglected but it is noticed by comparing with the results in [14] that their effect is negligible as is assumed in [14].

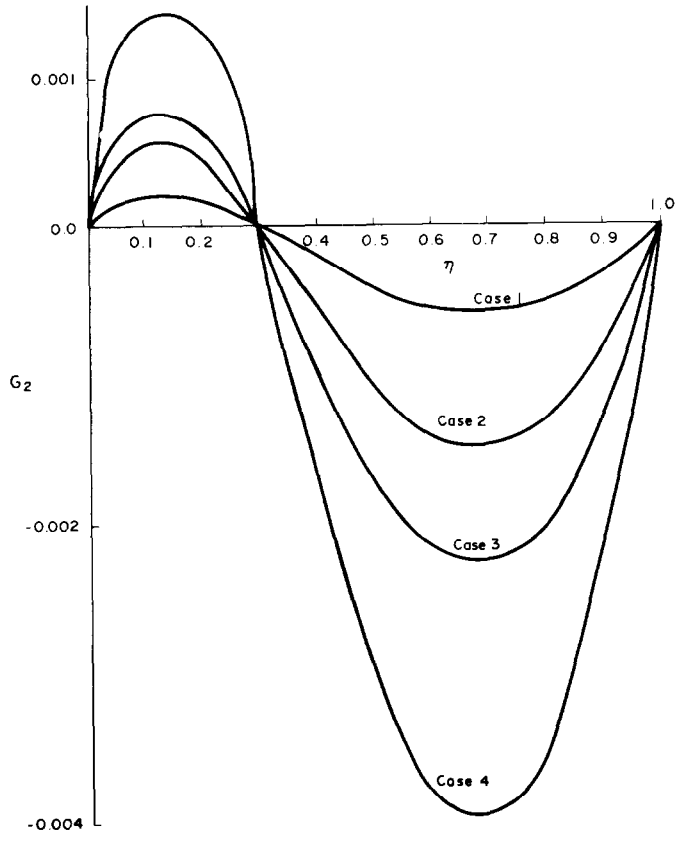
0.001
0.0
-0.002
-0.004
G_2
0.1
0.2
0.4
0.5
0.6
0.7
0.8
0.9
1.0
η
Case 1
Case 2
Case 3
Case 4

Fig. 5.

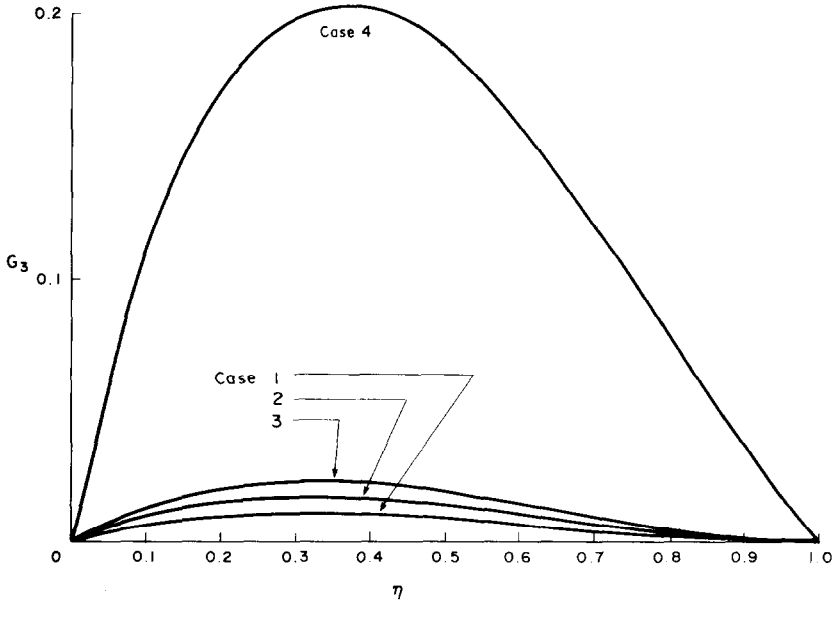
0.2
0.1
0
G_3
Case 4
Case 1
2
3
0.1
0.2
0.3
0.4
0.5
0.6
0.7
0.8
0.9
1.0
η

Fig. 6.

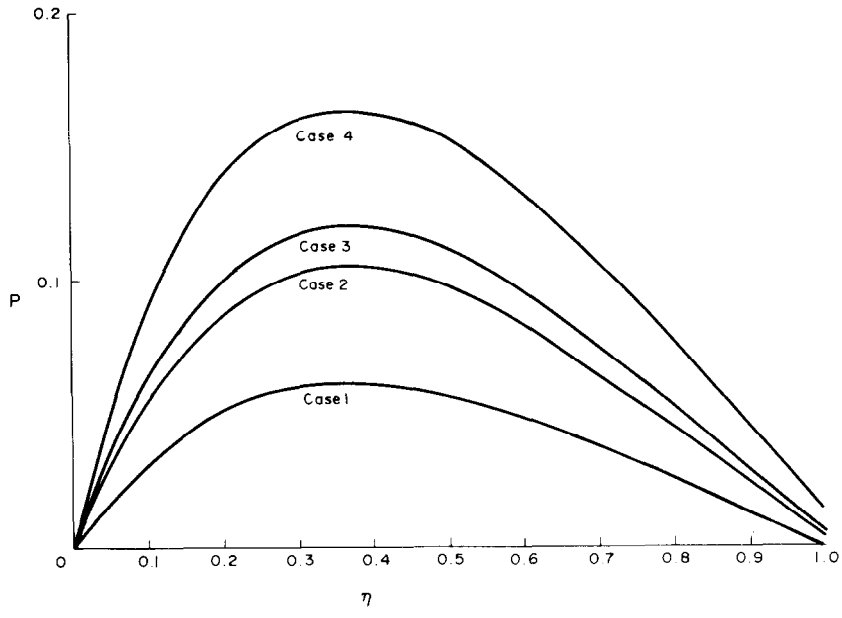

Fig. 7.

The micro-rotation (or spin) distributions are shown in Figs. 4–6. In Fig. 4, the symmetry of the spin component G_1 about the plane $\eta = 0.5$, where it has maximum value confirms the power series solution obtained by Datta and Sastry[14]. Figure 6 shows that the spin component G_3 is positive everywhere implying that it is in the same direction in which the disc rotates, also confirming the result given in [14]. Figure 7 shows the profile of the pressure which is positive everywhere indicates that it is maximum at the plane $\eta = 0.4$ and approaches to zero towards the upper plate.

REFERENCES

1. Th. Von Kármán, Über laminare und turbulente Reibung. *Z. Angew. Math. Mech.* **1**, 232–252 (1921).
2. W. G. Cochran, The flow due to a rotating disc. *Proc. Camb. Phil. Soc.* **30**, 365–375 (1934).
3. W. E. Milne, *Numerical Solution of Differential Equations*. Wiley, New York (1953).
4. E. L. Aero, A. N. Bulygin and E. V. Kuvshinskii, Asymmetric hydro-mechanics. *Appl. Math. Meth.* (PMM) **29**, 333–346 (1965).
5. A. C. Eringen, Theory of micropolar fluids. *J. Math. Mech.* **16**, 1–18 (1966).
6. D. W. Condiff and J. S. Dahler, Fluid mechanical aspects of anti-symmetric stress. *Phys. Fluids* **11**, 1919–1927 (1968).
7. J. D. Lee and A. C. Eringen, Wave propagation in nematic liquid crystals. *J. Chem. Phys.* **54**, 5027–5034 (1971).
8. Gurpal Singh and A. C. Smith, Flows of micropolar fluids with suction and injection. *Tensor, N.S.* **27**, 131–134 (1973).
9. C. F. Gerald, *Applied Numerical Analysis*. Addison-Wesley, Reading, Massachusetts (1974).
10. A. C. Smith and G. S. Guram, Kampé de Fériet and Taylor motions of a micropolar fluid. *Letters Appl. Engng Sci.* **2**, 279–292 (1974).
11. G. S. Guram and A. C. Smith, Micropolar flows with variable injection along a moving rigid wall. *Tensor, N.S.* **29**, 259–263 (1975).
12. G. S. Guram and A. C. Smith, Rectilinear pipe-flow of a micropolar fluid. *Utilitas Math.* **9**, 147–160 (1976).
13. A. C. Smith and G. S. Guram, Geometrical aspects of steady Ekman flow of a micropolar fluid. *Letters Appl. Engng Sci.* **5**, 215–227 (1977).
14. A. B. Datta and V. U. K. Sastry, Flow of a micropolar fluid between two infinite slowly rotating discs. *Z.A.M.M.* **57**, 113–115 (1977).
15. A. C. Smith, Some problems in generalised fluid dynamics, Third Canadian Symposium on Fluid Dynamics, University of Toronto, (5–8 June 1978).